$Co^{59}(p,\alpha)Fe^{56}$ and $Fe^{56}(p,p')$ Reactions*

H. K. VONACH AND J. R. HUIZENGA
Argonne National Laboratory, Argonne, Illinois
(Received 21 March 1966)

Evaporation spectra of α particles from the $Co^{59}(p,\alpha)Fe^{56}$ reaction and protons from the $Fe^{56}(p,p')$ reaction were investigated with silicon surface-barrier detectors for proton-bombarding energies of 9 to 13.5 MeV. The α-particle spectra are in good agreement with previous results. However, the proton spectra differ somewhat from earlier measurements. The anisotropy of the α particles from the $Co^{59}(p,\alpha)$ reaction was measured as a function of α-particle energy for proton-bombarding energies of 9 to 13.5 MeV. The level density and the spin-cutoff factor σ were calculated from the experimental results as a function of excitation energy in the range 3 to 9 MeV. The level density varies irregularly with excitation energy at the lower excitation energies and increases smoothly in an exponential manner at higher excitation energies. The nuclear temperature is in the range of 1.10 to 1.45 MeV and appears to increase slightly with excitation energy. The spin-cutoff factor σ increases from $3.5_{-0.3}{}^{+0.6}$ to $3.8_{-0.3}{}^{+0.5}$ in the excitation-energy range of 4 to 8 MeV.

I. INTRODUCTION

As part of a general investigation[1,2] of the levels in Fe^{56}, we have investigated the level density and spin-cutoff factor of Fe^{56} in the excitation-energy range of 3 to 9 MeV by study of the energy and angular distributions of particles emitted from the $Co^{59}(p,\alpha)$ and $Fe^{56}(p,p')$ reactions.

The main purpose of this paper is to present the experimental results and discuss some of the problems associated with calculations of level densities and spin-cutoff factors from energy and angular distributions of particles emitted in compound-nucleus reactions. A comparison of the level density of Fe^{56} determined in this experiment is made with results obtained in other experiments.

II. EXPERIMENTAL PROCEDURE

A. $Co^{59}(p,\alpha)Fe^{56}$ Reaction

Protons accelerated in the Argonne tandem Van de Graaff were used to bombard a metallic cobalt target foil of 1 mg/cm^2 thickness. Energy spectra of the emitted α particles were measured with surface barrier detectors which had energy resolutions of about 50 keV. The α-particle spectra at the two angles, 90° and 170°, were obtained simultaneously for six proton bombarding energies, 9.0, 10.0, 11.0, 12.0, 12.8, and 13.5 MeV. The target foil was positioned to bisect the angle between the two detectors. Hence, a different side of the target foil faced each detector and small shifts of the proton beam across the target did not introduce errors in the measured anisotropy. Distances of either 3 or 4 in. were used between the target and detectors. The bias on each of the solid-state detectors was adjusted to give a response depth equivalent to the range of the most energetic reaction α particles (16 MeV). With this operating condition the proton pulses were all below 5 MeV. Reaction deuterons and tritons were limited to energies of less than 5 MeV by Q-value restrictions.

A small amount of Cm^{244} was evaporated onto each side of the cobalt target foil. A comparison of the Cm^{244} α-particle counting rates at the two detectors gave the solid-angle ratio of the counters. In the present experiments the error in this ratio was less than 2%. An energy calibration with an accuracy of about 20 keV was obtained for each run from the positions of the 5.80-MeV natural α group of Cm^{244} and the reaction α-particle groups[3] leading to the ground and first excited state of Fe^{56} (see Fig. 1). A correction for energy loss in the target was made by adding an energy-dependent half-thickness of the target to the energy determined from the above calibration. The target thickness for 5.80-MeV α particles was measured directly by observing the difference in the positions of the Cm^{244} α lines from the front and back sides of the target foil (labeled α_1 and α_2, respectively, in Fig. 1). From this value and the known energy dependence of the stopping power[4] for α particles in cobalt metal, an energy-loss correction was computed for all energies. The Argonne 704 computer was used to make this energy-loss correction and to transform the data into a center-of-mass differential cross section as a function of the excitation energy of the residual nucleus Fe^{56}.

B. $Fe^{56}(p,p')$ Reaction

Energy spectra of the inelastically scattered protons were measured at 90° for five proton-bombarding energies, 9.5, 10.0, 10.5, 11.0, and 12.0 MeV. The inelastic protons are not expected to give measurable anisotropies[5] and, hence, no anisotropy measurements were included. The target was a metallic iron foil of

* Based on work performed under the auspices of the U. S. Atomic Energy Commission.
[1] H. K. Vonach and J. R. Huizenga, Phys. Rev. 138, B1372 (1965).
[2] A. A. Katsanos, J. R. Huizenga, and H. K. Vonach, Phys. Rev. 141, 1053 (1966).
[3] Since the reaction α-particle groups are broadened in energy because of energy loss in the target, the one-half peak-height point on the high-energy side of each peak was used in determining the α-particle energy.
[4] A. H. Wapstra, J. G. Nijgh, and R. Van Lieshout, *Nuclear Spectroscopy Tables* (North-Holland Publishing Company, Amsterdam, 1959).
[5] A. C. Douglas and N. MacDonald, Nucl. Phys. 13, 382 (1959).

0.53 mg/cm² thickness. The isotopic content of Fe^{56} in the target was greater than 99.8%. The protons were identified and their spectra measured with an dE/dx-E telescope consisting of thin and thick solid-state detectors. The energy resolution of the system was 200 keV. This poor energy resolution was due in part to the high noise level in the E detector at the large operating bias needed for stopping the most energetic protons.

III. RESULTS AND DISCUSSION

A. Energy Distributions of α Particles from the $Co^{59}(p,\alpha)$ Reaction

A typical α spectrum is illustrated in Fig. 1. These data are presented in terms of center-of-mass differential cross sections. The energy scale is given in both the laboratory α-particle energy and excitation energy in the residual nucleus Fe^{56}. The α particles populating the ground, first, and second excited states of Fe^{56} are resolved into peaks in the high-energy part of the α spectrum. In the low-energy part of the spectrum one observes the Cm^{244} α particles from the front (α_1) and back (α_2) sides of the target. The sharp rise in cross section in the region of the lowest particle energies is due to the onset of the protons.

The center-of-mass differential cross sections for α-particle emission at 90° are given in Table I as a function of excitation energy U in the residual nucleus Fe^{56} for six proton bombarding energies of 9.0, 10.0, 11.0, 12.0, 12.82, and 13.50 MeV. The excitation energy U ranges in each case from 2.5 MeV to an upper value fixed by the requirement that the reaction α particles exceed slightly the energy of the 5.80-MeV α particles of Cm^{244}. All cross sections reported in Table I are average values over 0.5-MeV energy intervals in the particle spectra. Since the target had a finite thickness (approximately 630 keV for 5.8-MeV alpha particles), Table I gives essentially all the information contained in the spectra. Statistical errors are less than 1% for cross sections exceeding 0.1 mb MeV^{-1} Sr^{-1} and less than 2% for all other cross sections. Relative values of the cross sections for a particular bombarding energy are believed to be accurate to ±3%. This error includes the statistical error and calibration errors discussed in Sec. II. Absolute cross-section values are determined to about ±10%. A large part of this error arises from an uncertainty in the effective target thickness (target thickness corrected for the angle subtended between the target and beam direction).

TABLE I. Center-of-mass differential cross sections in mb MeV^{-1} Sr^{-1} for α-particle emission in the reaction $Co^{59}(p,\alpha)Fe^{56}$ at 90° as a function of proton-bombarding energy E_p in the laboratory system and excitation energy U in the residual nucleus Fe^{56}.

U (MeV) \ E_p (MeV)	9.0	10.0	11.0	12.0	12.82	13.50
2.75	0.356	0.288	0.206	0.138	0.082	0.054
3.25	0.750	0.726	0.574	0.398	0.256	0.192
3.75	0.746	0.764	0.579	0.382	0.244	0.190
4.25	0.563	0.673	0.655	0.480	0.288	0.220
4.75	0.530	0.896	0.970	0.724	0.524	0.402
5.25	0.313	0.630	0.902	0.815	0.596	0.480
5.75		0.453	0.880	0.958	0.782	0.642
6.25			0.736	0.985	0.914	0.784
6.75			0.517	0.895	0.950	0.890
7.25				0.690	0.906	0.976
7.75				0.484	0.792	1.020
8.25					0.620	0.912
8.75					0.402	0.732
9.25						0.488

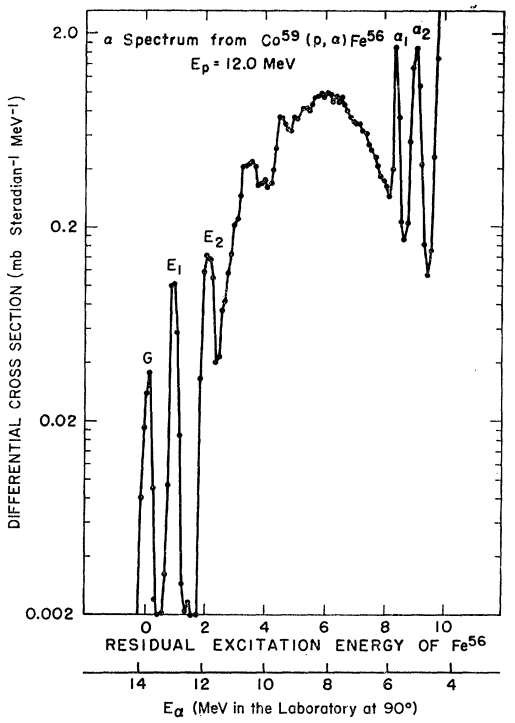

FIG. 1. Spectrum of α particles emitted at 90° in the $Co^{59}(p,\alpha)$-Fe^{56} reaction with 12-MeV (laboratory) protons. The α lines α_1 and α_2 originate from a Cm^{244} source evaporated onto the two sides of the cobalt foil.

For a reaction which proceeds by compound-nucleus formation, the level density $\rho(U)$ in the residual nucleus is related to the differential cross section $d^2\sigma/d\epsilon d\Omega$ for particle emission to that nucleus, assuming an infinite moment of inertia, by the relation[6]

$$d^2\sigma/d\epsilon d\Omega \propto \rho(U)\epsilon\sigma_c(\epsilon). \quad (1)$$

The quantity ϵ is the exit-channel energy corresponding to the excitation energy U in the residual nucleus (ϵ is sometimes defined as the total-disintegration energy or the sum of the center-of-mass kinetic energies of the emitted particle and recoil nucleus), and $\sigma_c(\epsilon)$ is the inverse cross section which is assumed equal to the cross section for formation of the compound nucleus at excitation energy U through a bombardment of the residual nucleus in its ground state by the emitted

[6] J. M. Blatt and V. F. Weisskopf, *Theoretical Nuclear Physics* (John Wiley & Sons, Inc., New York, 1952), p. 342.

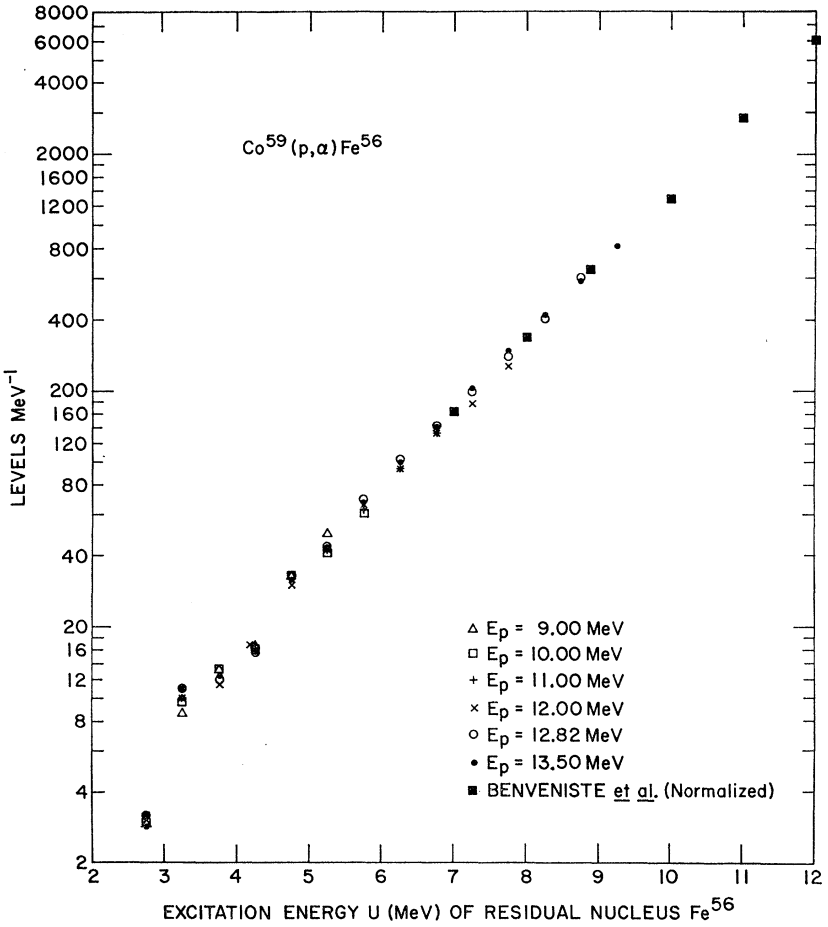

FIG. 2. Level density of Fe^{56} as a function of excitation energy U. Most of the data are calculated from α-particle spectra emitted in the $Co^{59}(p,\alpha)Fe^{56}$ reaction at different proton-bombarding energies. The absolute scale of the level density is obtained by a normalization described in the text in which $\int_{2.5}^{4.5}\rho(U)dU=21$. The squares are obtained from the $Fe^{56}(\alpha,\alpha')$ reaction for a bombarding energy of 21 MeV [Benveniste *et al.* (Ref. 11)] by normalizing to the $Co^{59}(p,\alpha)Fe^{56}$ data.

particle of channel energy ϵ. The channel energy ϵ of the emitted particle and the excitation energy U of the residual nucleus are related by

$$U=\epsilon_p-Q_0-\epsilon, \tag{2}$$

where ϵ_p is the bombarding energy of the projectile in the center-of-mass system and Q_0 is equal to $(M_{\text{emitted particle}}+M_{\text{residual nucleus}})-(M_{\text{projectile}}+M_{\text{target}})$ in units of energy.

Level densities of Fe^{56} were computed from the data of Table I and theoretical reaction cross sections[7] of α particles on Fe^{56}. Although no experimental data are available for Fe^{56}, the optical potential used gives good agreement with experimentally measured reaction cross sections for neighboring target nuclei.[8] From Eq. (1) one can calculate only relative values of the level density. However, the absolute level density was obtained by normalizing the level density in the excitation energy range 2.5 to 4.5 MeV, common to all spectra, to the known number of levels in this energy region determined by high-resolution magnetic spectroscopy.[2,9] Hence, for each bombarding energy the value of $\int_{2.5}^{4.5}\rho(U)dU$ was normalized to 21.[2,9] The resulting absolute value of the level density $\rho(U)$ as a function of excitation energy U of the residual nucleus Fe^{56} is shown in Fig. 2. Each point of Fig. 2 represents an average over an excitation-energy interval of 0.5 MeV. The data of Sherr and Brady[10] obtained from a study of the α-particle spectrum from the same reaction at a proton-bombarding energy of 17.6 MeV have essentially the same slope at the higher energies. We have included in Fig. 2 some data of Benveniste *et al.*[11] from the $Fe^{56}(\alpha,\alpha')$ reaction at a bombarding energy of 21 MeV. With inverse cross sections $\sigma_c(\epsilon)$ from the same source,[7] we have normalized their relative level-density data to our absolute scale.

From the results displayed in Fig. 2, we wish to emphasize the following points:

(a) The level density of Fe^{56} is obtained uniquely as a function of excitation energy, that is, the results are

[7] J. R. Huizenga and G. J. Igo, Nucl. Phys. **29**, 473 (1962); Argonne National Laboratory Report No. 6373, 1961 (unpublished).

[8] P. H. Stelson and F. K. McGowan, Phys. Rev. **133**, B911 (1964).

[9] M. H. Shapiro, P. F. Hinrichaen, R. Middleton, and R. K. Mohindra, Phys. Letters (to be published).

[10] R. Sherr and F. P. Brady, Phys. Rev. **124**, 1928 (1961).

[11] J. Benveniste, G. Merkel, and A. Mitchell, Phys. Rev. **141**, 980 (1966).

independent of the proton-bombarding energy. The points do scatter slightly with bombarding energy but no systematic deviation between the various level-density functions is recognizable. The irregular scatter of data, especially at the lower excitation energies, where only a few levels are contained in the 0.5-MeV averaging interval, is due partly to Ericson fluctuations. The target thickness of 40 keV for bombarding protons is insufficient for the fluctuations to average out completely.[12] The good agreement between the level densities obtained at the different bombarding energies, indicates that this reaction is adequately described by the statistical theory in the energy range investigated, and that the reaction cross sections $\sigma_c(\epsilon)$ calculated from the ground-state target nucleus (optical potential) remain valid for higher excitation energies.

(b) In the excitation energy range of 2 to 5 MeV in Fe^{56}, the level density shows a definite structure which is very similar to that obtained by direct level counting with the high-resolution magnetic spectrograph.[2]

(c) At the higher excitation energies, our results are in good agreement with those of Sherr and Brady,[10] and are qualitatively consistent with a simple exponential increase of the level density with increasing excitation energy (a constant-temperature-type level density). For the excitation-energy range 5 to 9.5 MeV investigated in these experiments, we derive from Fig. 2 a nuclear temperature T of 1.37 ± 0.05 MeV. This is smaller than the temperature of 1.54 MeV determined by Sherr and Brady[10] for the excitation-energy range 7 to 13 MeV. A constant-temperature-type level density with $T\approx1.45$ MeV gives an approximate representation of the level density over the excitation-energy range 5 to 13 MeV. On a quantitative basis, however, these results indicate that the temperature is increasing with excitation energy.

Equation (1) is valid only when the spin dependence of the level density has the form

$$\rho(U,J)=(2J+1)\rho(U,0). \quad (3)$$

Actually the spin dependence of the level density is given by[13]

$$\rho(U,J)=(2J+1)\rho(U,0)\exp\{-J(J+1)/2\sigma^2\}, \quad (4)$$

where σ is the spin-cutoff factor which is related to the nuclear moment of inertia $\mathcal{I}$ and temperature t by the relationship $\sigma^2=\mathcal{I}t/\hbar^2$. As mentioned previously, if the moment of inertia is assumed infinite, Eq. (4) reduces to Eq. (3) and Eq. (1) becomes valid. A theoretical equation has been derived[5,14] which gives the differential cross section for particle emission when the spin dependence of Eq. (4) is included. [See Eq. (A1) of Appendix I.] In the treatment of experimental data one seeks to know the conditions for which Eq. (1) is a sufficiently good approximation. Thomas[15] has investigated this question for inelastic neutron scattering and found only a small difference between the results calculated with Eq. (1) and Eq. (A1). A similar comparison is of practical interest for other types of reactions also since the use of Eq. (1) results in a considerable simplification of the calculations. The results of a number of numerical calculations with Eqs. (1) and (A1) are compiled and discussed in Appendix II.

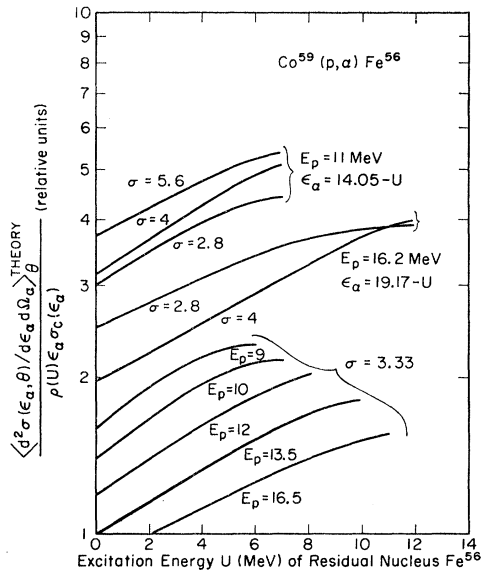

FIG. 3. Deviation of evaporation spectra calculated with exact-statistical and approximate theories [see Eq. (A2)] for the $Co^{59}(p,\alpha)Fe^{56}$ reaction. The values of the ordinate for different cases were shifted for ease of display and hence the absolute values are of no significance.

The results of interest for the $Co^{59}(p,\alpha)Fe^{56}$ reaction are shown in Fig. 3. The value of $A(\epsilon)$, which is defined in Appendix II, increases with excitation energy U [related to the channel energy ϵ of the emitted particle by Eq. (2)] and demonstrates a sizable angular-momentum effect. However, the deviations between Eq. (1) and Eq. (A1) depend only weakly on bombarding energy and spin-cutoff factor σ. Therefore, the comparison of level densities calculated from α spectra at different bombarding energies but at the same excitation energy U remains valid. The change in level density with excitation energy derived from the use of Eq. (1) is not strictly valid. The results of Fig. 3 indicate that the nuclear temperature from the $Co^{59}(p,\alpha)$ reaction should be increased by about 5% to a value of 1.44 MeV.

B. Energy Distributions of Protons from the $Fe^{56}(p,p')$ Reaction

A typical proton spectrum from the present measurements is shown in Fig. 4. All spectra contain a low-

[12] H. K. Vonach, A. A. Katsanos, and J. R. Huizenga, Phys. Rev. Letters **13**, 88 (1964).
[13] T. Ericson, Advan. Phys. **9**, 425 (1960).
[14] W. Hauser and H. Feshbach, Phys. Rev. **87**, 366 (1952).
[15] T. D. Thomas, Nucl. Phys. **53**, 558 (1964).

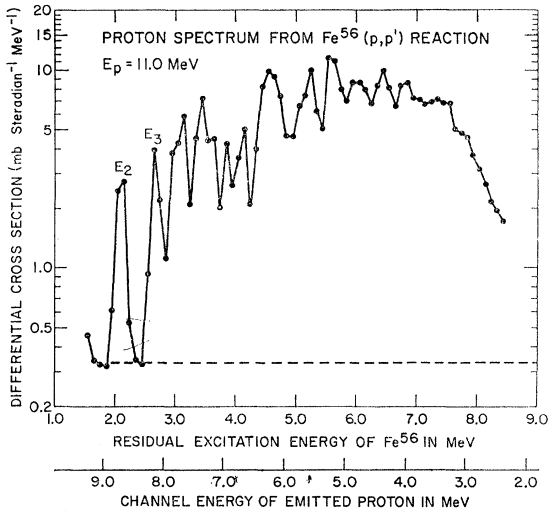

FIG. 4. Spectrum of protons inelastically scattered from Fe^{56} at 90° with a proton-bombarding energy of 11 MeV (laboratory). The peaks E_2 and E_3 refer to the second and third excited levels in Fe^{56}.

energy tail of the elastic peak. This can be seen in Fig. 4, where the intensities in the minima between the isolated peaks on the right side of the figure are finite. This background was confirmed also in measurements of spectra of protons scattered from carbon and gold, where the magnitude of the background was found to be almost independent of proton energy. The spectra were all corrected for this effect by subtracting a constant background equal to the intensity observed in the minimum between the second and third excited levels of Fe^{56} (see Fig. 4).

Center-of-mass differential cross sections for inelastic proton scattering on Fe^{56} at 90° are given in Table II for proton-bombarding energies of 9.5, 10.0, 10.5, 11.0, and 12.0 MeV. The cross sections are averaged over 0.5-MeV excitation-energy intervals and corrected for the "elastic background" as described above. Because of the uncertainty of this background correction, relative cross sections are believed to be accurate to 5% and absolute cross sections to about 12%.

TABLE II. Center-of-mass differential cross sections (mb MeV^{-1} Sr^{-1}) for inelastic proton scattering on Fe^{56} at 90° as a function of proton-bombarding energy E_p in the laboratory system and excitation energy U in the residual nucleus.

U (MeV) \ E_p (MeV)	9.5	10.0	10.5	11.0	12.0
2.75	4.26	3.44	2.84	2.24	1.32
3.25	8.06	5.30	5.60	4.56	2.68
3.75	7.26	5.76	5.90	3.12	2.52
4.25	7.60	6.36	5.68	4.44	2.92
4.75	8.88	8.30	8.30	6.90	5.26
5.25	7.30	6.90	6.94	6.52	4.88
5.75	6.64	6.90	9.16	8.69	6.00
6.25	4.20	6.08	8.20	8.04	7.04
6.75	2.12	4.22	7.10	7.44	7.90
7.25		2.04	4.30	6.40	7.38
7.75			2.90	4.42	6.86
8.25				1.92	5.78
8.75					3.62

Spectra of inelastically scattered protons from iron have been measured previously by Cohen and Rubin[16] for incident proton energies of 11 to 23 MeV. In Fig. 5 Cohen and Rubin's spectrum[16] at a proton-bombarding energy of 11.3 MeV is compared with our spectrum at an incident energy of 11.0 MeV. Each point of our spectrum is averaged over an energy interval of 1 MeV in order to simulate better the experimental resolution of Cohen and Rubin.[16] Even so, the present spectrum after averaging over 1-MeV intervals, shows more structure than that of Cohen and Rubin[16] and indicates that their energy resolution is larger than 1 MeV. The proton intensities on both sides of the broad maximum

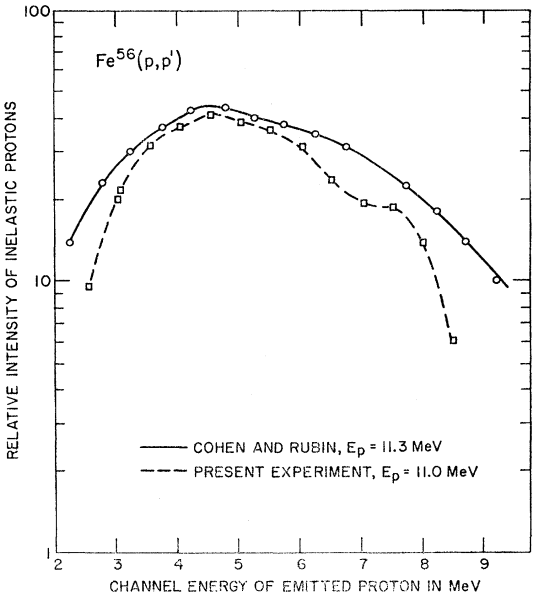

FIG. 5. Comparison of the present $Fe^{56}(p,p')$ results with those of Cohen and Rubin (Ref. 16). Both measurements were made at 90°. Each point of the present experiment is averaged over an energy interval of 1 MeV.

of our spectrum decrease much more rapidly than that of Cohen and Rubin[16] as can be seen in Fig. 5. Part of this discrepancy may be due to the apparent neglect of a correction for the low-energy tail of the elastic peak. In addition, protons scattered elastically may not have been discriminated from protons scattered inelastically in the older measurements[16] because of the poorer energy resolution. Since these uncertainties exist in the previous measurements, analyses of the existing data in terms of level densities will be restricted to the present measurements.

Level densities are computed with Eq. (1) since the angular-momentum effects for the $Fe^{56}(p,p')$ reaction are shown to be negligible in Appendix II. The inverse

[16] B. L. Cohen and A. G. Rubin, Phys. Rev. **113**, 579 (1959).

cross sections were computed with the optical potential of Perey.[17] As described earlier in Sec. III(A), the number of levels in Fe^{56} in the excitation-energy range 2.5 to 4.5 MeV, $\int_{2.5}^{4.5}\rho(U)dU$, was normalized to 21 for each proton-bombarding energy. The level densities calculated from the proton spectra at different bombarding energies are plotted in Fig. 6 and agree rather well for the lower excitation energies (higher energies of emitted protons). Small deviations occur in the level densities calculated from the different spectra for high excitation energies (low energies of emitted protons). These deviations occur for excitation energies corresponding to inelastic proton energies in the range of 2.5 to 4 MeV (see Fig. 6). These results indicate that the inverse reaction cross section in Eq. (1) should drop less steeply with energy in this energy range than is predicted by the Perey optical potential.

The general features of the level densities calculated from the (p,p') spectra are in reasonable agreement with those calculated from the (p,α) spectra. The structure in the level density as a function of energy in the 2.5 to 6.0 MeV energy range of Fig. 2 is well reproduced in Fig. 6. The proton data are consistent with a constant-temperature-type level density over a small range in excitation energy. For an excitation-energy range 4.5 to 7 MeV, the nuclear temperature is 1.25±0.05 MeV.

Level densities computed from the inelastic neutron spectrum of Thomson[18] for the $Fe^{56}(n,n')$ reaction with 7-MeV neutrons are plotted also in Fig. 6. Thomson's data[18] were corrected for the inverse cross sections calculated with the optical potential of Bjorklund and Fernbach[19,20] and normalized to the $Fe^{56}(p,p')$ data.

Structure in the level density of Fe^{56} as a function of excitation energy obtained from the $Fe^{56}(n,n')$ data is very similar to the charged-particle data. The nuclear temperature is also the same as that obtained from the $Fe^{56}(p,p')$ data.

C. Anisotropy of α Particles from the $Co^{59}(p,\alpha)Fe^{56}$ Reaction

In Table III experimental values of the anisotropy, defined as $[\sigma(170°)/\sigma(90°)]-1$, for α particles emitted in the $Co^{59}(p,\alpha)Fe^{56}$ reaction are summarized. Values of the anisotropy are given both as a function of proton-bombarding energy E_p and excitation energy U of the residual nucleus Fe^{56}. The numerical values listed are averages over excitation-energy ranges of 1 MeV except in the lowest excitation-energy range (3–5 MeV), where the average is over 2 MeV. Further subdivision of the data in the latter energy interval gives no additional information since the number of levels contained in this energy interval is rather small, and when only a few levels are contributing to the anisotropy it varies rapidly and irregularly due to Ericson fluctuations. Even with all the levels in a 2-MeV energy bin in the 3 to 5 MeV excitation-energy range, fluctuations in the anisotropy appear to occur (see Fig. 7). The ratio $\sigma(170°)/\sigma(90°)$ is accurate to about 3%. This error is a composite of the solid-angle ratio of the two counters (2%), the error in the energy calibration (2%), and the statistical error in the cross-section ratio (1%). Values of the anisotropies are consequently accurate to ±0.03.

For compound-nucleus reactions, the differential cross sections are expected theoretically (Appendix I) to be symmetrical about 90° to the projectile direction. Isotropic distributions will occur only if the level density of the residual nucleus has a simple spin dependence[5,13] of Eq. (3) which corresponds to the spin-cutoff parameter σ taking on an infinite value. For the spin dependence of the level density given by Eq. (4) with a finite value of σ, the statistical theory predicts an angular

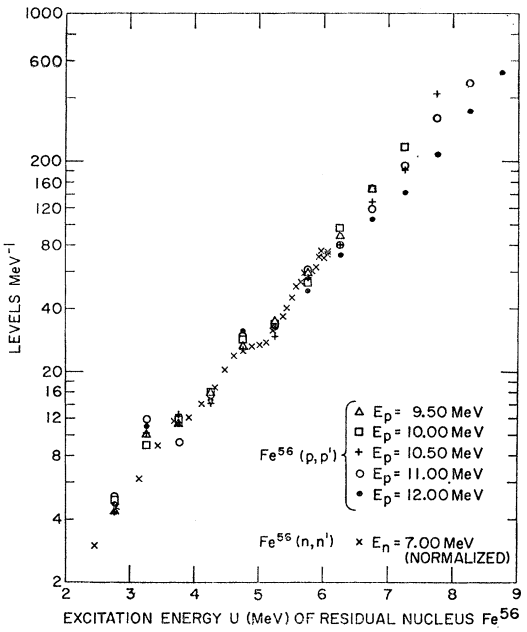

FIG. 6. Level density of Fe^{56} as a function of excitation energy U. The absolute scale of the level density is obtained by a normalization described in the text in which $\int_{2.5}^{4.5}\rho(U)dU=21$. The crosses (×) are obtained from the $Fe^{56}(n,n')$ reaction with 7-MeV bombarding energy [Thomas (Ref. 18)] by normalizing to the $Fe^{56}(p,p')$ data.

TABLE III. Anisotropy ($[\sigma(170°)_{c.m.}/\sigma(90°)_{c.m.}]-1$) of α particles emitted in the $Co^{59}(p,\alpha)Fe^{56}$ reaction as a function of proton-bombarding energy E_p in the laboratory system and excitation energy U in the residual nucleus Fe^{56}.

U (MeV) \ E_p (MeV)	9.0	10.0	11.0	12.0	12.82	13.5
3–5	0.05	0.115	0.075	0.125	0.25	0.21
5–6		0.065	0.100	0.090	0.090	0.15
6–7			0.065	0.065	0.100	0.087
7–8					0.120	0.047
8–9						0.080

[17] F. G. Perey, Phys. Rev. **131**, 745 (1963).
[18] D. B. Thomson, Phys. Rev. **129**, 1649 (1963).
[19] F. Bjorklund and S. Fernbach, Phys. Rev. **109**, 1295 (1958).
[20] E. H. Auerbach and F. G. Perey, Brookhaven National Laboratory Report No. 765, 1962 (unpublished).

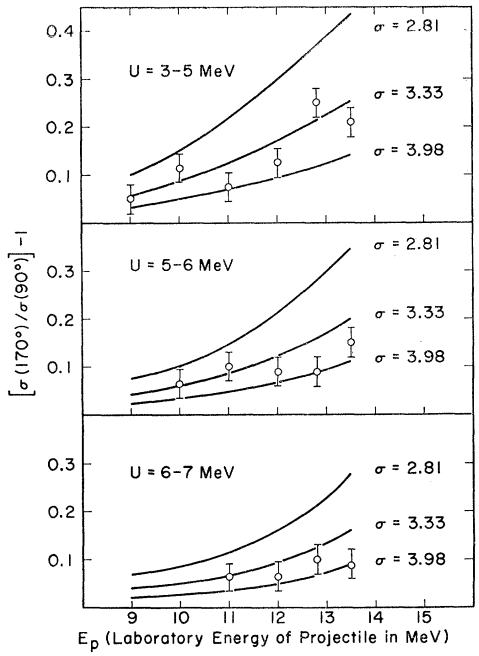

FIG. 7. Comparison of the experimentally determined anisotropy of α particles emitted in the $Co^{59}(p,\alpha)Fe^{56}$ reaction with theoretical values for different values of the spin-cutoff factor σ.

distribution which is symmetric about and containing a minimum at 90° and maxima at 0° and 180°. The magnitude of the anisotropy depends on σ, and consequently the spin-cutoff parameter σ can be determined from experimental measurements of the anisotropy.

By making a number of approximations, Ericson and Strutinskii[21] derived a rather simple expression for the angular dependence of the differential cross section, namely,

$$\frac{d^2\sigma_{ab}(\epsilon_b,\theta)}{d\epsilon_b d\Omega_b} = \text{const}\left\{1+\frac{1}{12}\frac{\langle l_a^2(\epsilon_a)\rangle\langle l_b^2(\epsilon_b)\rangle}{\sigma^4(U)}P_2(\cos\theta)\right\}, \quad (5)$$

where $\langle l_a^2(\epsilon_a)\rangle$ and $\langle l_b^2(\epsilon_b)\rangle$ are the mean-square-orbital angular momenta of the bombarding and emitted particle, respectively. The mean-square-orbital angular momenta are defined by the relation

$$\langle l^2(\epsilon)\rangle = \sum_0^\infty l^3 T^l(\epsilon) / \sum_0^\infty l T^l(\epsilon),$$

where $T^l(\epsilon)$ are the optical-model transmission coefficients for either the bombarding (subscript a) or the emitted (subscript b) particles. In the derivation of Eq. (5) the spins of all the reaction particles are neglected. Since only the $P_2(\cos\theta)$ term is retained, Eq. (5) is expected to be valid only for small values of the anisotropy, $[(\sigma(180°)/\sigma(90°))-1] \ll 1$. Ericson and Strutinskii assumed the total width of the compound levels Γ_J to be independent of angular momentum J and performed the calculation in the classical limit.

The exact result of the statistical theory of nuclear reactions for the angular dependence of the differential cross section is given by Douglas and MacDonald.[5] Their differential cross section is given also in terms of Legendre polynomials (see Appendix I). In this case, however, the coefficients $B_{2L}(\epsilon_b)$ are complicated functions of the transmission coefficients $T_a{}^l(\epsilon_a)$ and $T_b{}^l(\epsilon_b)$ of the bombarding and emitted particles, respectively, spins of all reaction particles, level densities, and spin-cutoff parameters σ of all residual nuclei. The explicit expression for $B_{2L}(\epsilon_b)$ in terms of the above parameters is given in Appendix I.

Some of the experimental anisotropies tabulated in Table III are compared with the exact predictions of statistical theory in Fig. 7. Details of the theoretical calculations are described in Appendix I. Additional calculations were performed to study the dependence of the anisotropy on the various parameters and to compare the exact results with the approximate predictions of Eq. (5). These results are reported in Appendix I. In each of the Figs. 7(a), 7(b), and 7(c), the anisotropies for the same excitation-energy range in the residual nucleus from several different proton bombarding energies are compared with theoretical predictions for a variety of spin-cutoff factors. Since σ is expected to be a function of excitation energy in the residual nucleus, the experimental anisotropy values for a fixed excitation energy should be confined (within experimental error) to a curve with σ equal to a constant.

The experimental anisotropies in Fig. 7 scatter somewhat more than expected from the experimental errors (especially in the 3 to 5 MeV excitation-energy range). A considerable part of the irregular fluctuations of the

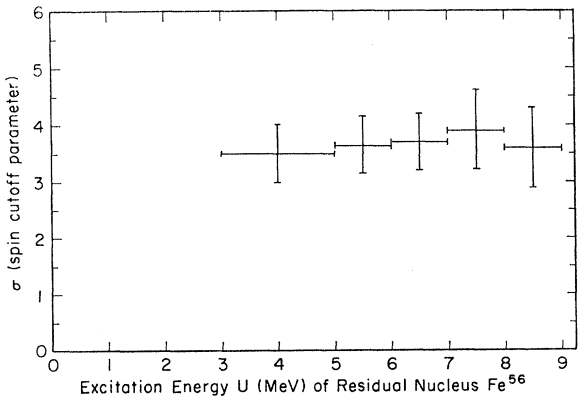

FIG. 8. Comparison of theoretical values for the anisotropy of α particles emitted in the $Co^{59}(p,\alpha)$ reaction for a proton-bombarding energy of 12 MeV (laboratory) and three values of the spin-cutoff parameter σ.

[21] T. Ericson and V. M. Strutinskii, Nucl. Phys. 8, 284 (1958).

experimental anisotropy values around the theoretical line with constant σ is undoubtedly due to Ericson fluctuations. The excitation-energy ranges 3 to 5 and 5 to 6 MeV contain approximately 30 and 50 levels, respectively. Hence, we can estimate from measurements of cross-section fluctuations for formation of single levels[12] that variations in the anisotropy of 2 to 3% are expected for these energy ranges and a target thickness of 40 keV.

The energy dependence of the spin-cutoff factor σ is shown in Fig. 8. Values of σ for the various energy ranges were determined from the data of Fig. 7(a), 7(b), and 7(c) and comparison of the remaining results of Table III (not included in Fig. 7) with theory. The errors in the spin-cutoff factor σ which are shown in Fig. 8 were estimated from the scattering of the experimental data of Fig. 7, the experimental errors and the theoretical dependence of the anisotropy on σ. The possibility of additional systematic errors due to contributions of direct interactions to the angular distributions cannot be excluded completely. However, it is not clear at present how the amount of direct interaction and its angular distribution in the region of backward angles can be estimated from the measured angular distribution. However, the fact that σ does not appear to depend systematically on the bombarding energy indicates that the systematic error from the contribution of direct interaction is rather small.

APPENDIX I: STATISTICAL-THEORY CALCULATION OF THE ANISOTROPY OF α PARTICLES FROM THE $Co^{59}(p,\alpha)Fe^{56}$ REACTION

The energy and angular distributions of particles emitted in a compound-nuclear reaction are given according to Douglas and MacDonald[5] by

$$\frac{d^2\sigma_{ab}(\epsilon_b,\theta)}{d\epsilon_b d\Omega_b}=\sum_{L=0}^{\infty} B_{2L}(\epsilon_b)P_{2L}(\cos\theta). \qquad \text{(A1)}$$

The function $B_{2L}(\epsilon_b)$ is

$$B_{2L}(\epsilon_b)=(2I_a+1)^{-1}(2i_a+1)^{-1}k_a^{-2}\sum_{S_a,S_b,I_b}\sum_{l_a,l_b,J}\frac{(-1)^{S_a-S_b}T_a^{l_a}(\epsilon_a)T_b^{l_b}(\epsilon_b)Z(l_aJl_aJ;S_aL)Z(l_bJl_bJ,S_bL)\rho_b(U_b,I_b)}{4\sum_{b'}\int_0^{U_{b'\max}}dU_{b'}\sum_{l=0}^{l_{\max}}T_{b'}^{l_{b'}}(\epsilon_{b'})\sum_{S_{b'}=|J-l_{b'}|}^{J+l_{b'}}\sum_{I_{b'}=|S_{l'}-i_{l'}|}^{S_{b'}+i_{b'}}\rho_{b'}(U_{b'},I_{b'})},$$

where I_a, i_a, J, I_b, and i_b are the spins of the target, projectile, compound nucleus, residual nucleus, and emitted particle, respectively; S_a and S_b are the channel spins in the incident and outgoing channels, respectively; l_a and l_b are the orbital angular momenta of the incident and outgoing particles, respectively; k_a is the wave number of the incident particles; $P_L(\cos\theta)$ is the Legendre polynomial of order L; $T_a^{l_a}(\epsilon_a)$ and $T_b^{l_b}(\epsilon_b)$ are transmission coefficients for the projectile and the emitted particle, respectively, with total energies in the center-of-mass systems (channel energies) of ϵ_a and ϵ_b; $Z(l_aJl_aJ,S_aL)$ and $Z(l_bJl_bJ,S_bI)$ are the so-called Z coefficients for the random sign assumption (implies that $2L$ is even and that the angular distribution is symmetric about 90°) and are defined as sums of products of Racah and Clebsch-Gordan coefficients[5]; $\rho_b(U_b,I_b)$ is the energy- and spin-dependent level density of the residual nucleus formed by the emission of particle b with channel energy ϵ_b; and the sum over b' refers to the sum over all the different types of emitted particles.

The summation in the numerator of $B_{2L}(\epsilon_b)$ can be performed independently with respect to the quantum numbers l_a, l_b, J, and I_b since the Z coefficients vanish for combinations of the quantum numbers which violate the conservation of angular momentum. The sums over channel spins S_a and S_b have to be performed from $|I_a-i_a|$ to $|I_a+i_a|$ and $|I_b-i_b|$ to $|I_b+i_b|$, respectively. The first term of the sum over L in Eq. (A1) gives the energy distribution averaged over solid angle, since the contribution of the higher Legendre polynomials vanishes when they are integrated over solid angle, owing to their orthogonality. A FORTRAN program for numerical evaluation of Eq. (A1) was developed by Dr. H. Bowsher and Dr. M. Halbert and was used by the authors with minor modifications. The program computes the quantities $B_{2L}(\epsilon_b)$ for values of ϵ_b which correspond to excitation energies U_b in the residual nucleus of zero to the maximum excitation energy allowable in 0.5-MeV steps. Calculations are performed for $L=0$, 1, 2, and 3; however, the coefficient B_6 was negligible for all calculations performed.

In the sums over l_a, l_b, $l_{b'}$, and J, values up to 17 were included in each sum. Values up to 15 were included in the sums over I_b and $I_{b'}$. The integrals in the denominator of $B_{2L}(\epsilon_b)$ were approximated by sums. The integrands were calculated at points 0.5 MeV apart and the integral computed from these values according to Simpson's rule.

The transmission coefficients $T_a^{l_a}(\epsilon_a)$, $T_b^{l_b}(\epsilon_b)$, and $T_{b'}^{l_{b'}}(\epsilon_{b'})$ for the projectile and emitted particles (only neutrons, protons, and α particles are included; deuteron emission is negligible for this case) were computed with the ABACUS II optical-model program. Optical-model parameters of Bjorklund and Fernbach,[19] Perey,[17] and Huizenga, and Igo[7] were employed in the calculations of transmission coefficients for neutrons, protons, and α particles, respectively. A constant temperature

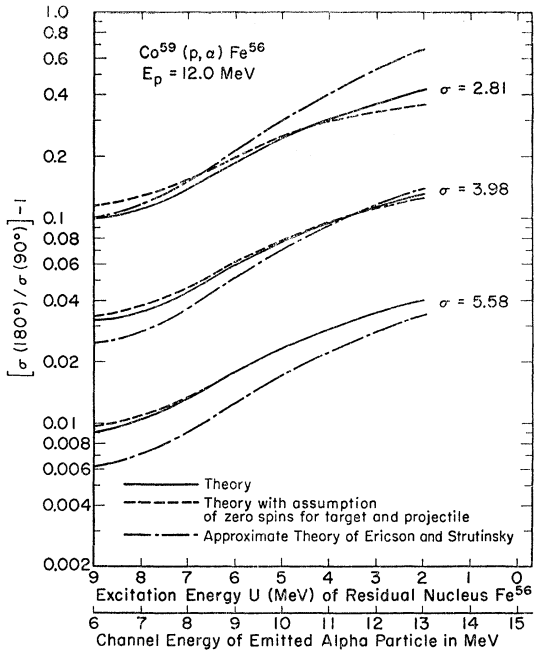

FIG. 9. Energy dependence of the spin-cutoff parameter σ.

and a constant spin-cutoff-type level density were assumed for the residual nucleus. A nuclear temperature of 1.4 MeV was used.

With the above assumptions the differential cross sections for emission of α particles in the $Co^{59}(p,\alpha)Fe^{56}$ reaction were computed. The results are shown in Fig. 7. The anisotropy of the emitted α particles $[(\sigma_{170°}/\sigma_{90°})-1]$ is plotted as a function of proton-bombarding energy for each of three excitation-energy regions in the residual nucleus, $U=3$–5, 5–6, and 6–7 MeV. Theoretical calculations were performed also to study the influence of target and projectile spins on the anisotropy. Theoretical anisotropies for α particles emitted in the $Co^{59}(p,\alpha)Fe^{56}$ reaction for a proton-bombarding energy of 12 MeV were computed with Eq. (A1) and the Ericson-Strutinskii approximation [Eq. (5)] as a function of α-particle energy for three different spin-cutoff factors, $\sigma=2.81$, 3.98, and 5.58. It can be seen in Fig. 9 that the results obtained with the approximate Eq. (5) of Ericson and Strutinskii agree approximately with the exact calculations of the anisotropy $[(\sigma_{180°}/\sigma_{90°})-1]$ in the range 0.02 to 0.2. Although these results were obtained for a specific case, similar results were obtained for a number of other cases also. The anisotropy and the difference between the results obtained with the exact and approximate theories depend essentially on the mean-square-orbital angular momentum of the projectile and emitted particle and the spin-cutoff parameter σ of the residual nucleus. The comparisons shown in Fig. 9 cover a range of values for σ of 2.8 to 5.6 and a range of values for the mean-square-orbital angular momentum of 6 to 30 for the emitted α particles. It was not necessary to vary the orbital angular momentum of the projectile, since Eqs. (5) and (A1) are symmetric with respect to the transmission coefficients of the projectiles and emitted particles. Hence, the results of Fig. 9 are valid also for projectiles with mean-square-orbital angular momenta of 6 to 30. We conclude that the approximate equation of Ericson and Strutinskii is sufficiently accurate to analyze anisotropy data for reactions meeting the criteria stated above for the data of Fig. 9.

The theoretical dependence of the anisotropy on target and projectile spin is very weak. This is shown in Fig. 9 for the reaction $Co^{59}(p,\alpha)Fe^{56}$. The anisotropy is computed with Eq. (A1) with the assumption that the target and projectile spins are 0 (actually $\frac{7}{2}$ and $\frac{1}{2}$, respectively). The good agreement between these anisotropies and those from the exact calculation (including the target and projectile spins) is shown in Fig. 9. Similar results were obtained for the $Co^{59}(p,\alpha)Fe^{56}$ reaction with projectiles of other energies and for the $Fe^{56}(\alpha,\alpha')$ reaction when comparing results for target spins 0 and 4. If calculations of anisotropy are to be made with Eq. (A1), a great saving in computing time is accomplished with only a small loss in the accuracy of the results by neglecting the spins of the projectile and target.

APPENDIX II: THEORETICAL DISTRIBUTIONS OF PARTICLES EMITTED IN A COMPOUND-NUCLEUS REACTION: COMPARISON OF THE EXACT STATISTICAL THEORY (ANGULAR MOMENTUM INCLUDED) AND THE APPROXIMATE THEORY

[ASSUMES $\rho(U,J)=(2J+1)\rho(U,0)$]

With only minor changes, the program described in Appendix I was used for computing the exact results of the statistical theory taking into account angular-momentum effects. The modified program calculated the quantity $A(\epsilon)$,

$$A(\epsilon)=\langle d^2\rho(\epsilon,\theta)/d\epsilon d\Omega\rangle_\theta/\rho(U)\epsilon\sigma_C(\epsilon)\,, \qquad \text{(A2)}$$

where $\langle d^2\sigma(\epsilon,\theta)/d\epsilon d\Omega\rangle_\theta$ is the theoretical differential cross section of Eq. (A1), for particle emission with channel energy ϵ, averaged over solid angle $[B_0(\epsilon)$ of Eq. (A1)]. The quantities $\rho(U)$, ϵ, and $\sigma_c(\epsilon)$ are the same as those defined in Eq. (1). If Eq. (1) were strictly valid, $\langle d^2\sigma(\epsilon,\theta)/d\epsilon d\Omega\rangle_\theta$ would be proportional to the quantity $\rho(U)\epsilon\sigma_c(\epsilon)$ and $A(\epsilon)$ would be a constant factor.

The rate of change in the factor $A(\epsilon)$ with the channel energy ϵ of the emitted particle is used as a measure of the magnitude of the deviation between the exact results of the statistical theory and the Weisskopf approximation[6] given by Eq. (1). The magnitude of these deviations depends mostly on the average orbital angular momenta of the bombarding and emitted particles (therefore, on the masses and energies of these particles) and the spin-cutoff parameter σ of the residual

nucleus. The quantity $A(\epsilon)$ was calculated as a function of ϵ for a number of values of the above-mentioned parameters. The transmission coefficients were computed with the optical-model parameters given in Appendix I. The form of the energy dependence of the level density was also that given in Appendix I. The bombarding energy, types of bombarding and emitted particles, and spin-cutoff parameter σ were varied in the calculations.

The results of the calculations in terms of the change in $A(\epsilon)$ as a function of excitation energy U of the residual nucleus for the reactions $Co^{59}(p,\alpha)$ and $Fe^{56}(\alpha,\alpha')$ are shown in Figs. 3 and 10 for various values

TABLE IV. Numerical values of the deviation of evaporation spectra calculated with the exact-statistical and approximate theories [see Eq. (A2)].

Reaction	Bombarding energy (MeV)	Spin-cutoff parameter of residual nucleus	Excitation-energy range (MeV)	$\left\langle \frac{1}{A(\epsilon)} \frac{dA(\epsilon)}{dU} \right\rangle$
$Fe^{56}(\alpha,\alpha')$	13.74	2.8	2– 8	−0.018
	20.40	2.8	–14	−0.112
	20.40	4.0	–6.5	−0.015
(α,p)	13.74	2.8	–6.5	−0.008
	13.74	4.0	–6.5	−0.008
	20.40	2.8	–12.5	−0.051
	20.40	4.0	–12.5	−0.007
(α,n)	13.74	2.8	–6.5	−0.009
	13.74	4.0	–6.5	−0.010
	20.40	2.8	–12.5	−0.058
	20.40	4.0	–12.5	−0.007
(p,p')	11.0	2.8	–8.0	0.032
	11.0	4.0	–8.0	0.021
(n,α)	7.32	2.8	–5.0	0.064
	7.32	3.72	–5.0	0.047
(n,p)	7.32	2.8	–5.5	0.026
	7.32	3.72	–5.5	0.020
(n,n')	7.32	2.8	–6.0	0.033
	7.32	3.72	–6.0	0.025
$Co^{59}(p,\alpha)$	9.0	3.33	–7.0	0.037
	10.0	3.30	–8.0	0.043
	11.0	2.8	–8.5	0.031
	11.0	4.0	–9.0	0.047
	11.0	5.6	–8.5	0.027
	12.0	3.33	–10.0	0.047
	13.5	3.30	–11.5	0.047
	16.2	2.8	–14.0	0.026
	16.2	4.0	–14.0	0.048
(p,p')	9.0	3.33	–5.5	0.014
	10.0	3.30	–6.5	0.013
	11.0	2.8	–7.5	0.007
	11.0	4.0	–7.5	0.017
	11.0	5.6	–7.5	0.009
	12.0	3.33	–8.5	0.012
	13.5	3.30	–10.0	0.019
	16.2	2.8	–12.5	0.001
	16.2	4.0	–12.5	0.012
$Co^{59}(p,n)$	9.0	3.33	–5.5	0.019
	10.0	3.30	–5.6	0.018
	11.0	2.8	–7.5	0.011
	11.0	4.0	–7.5	0.016
	11.0	5.6	–7.5	0.013
	12.0	3.33	–8.5	0.016
	13.5	3.30	–10.0	0.025
	16.2	2.8	–12.5	0.003
	16.2	4.0	–12.5	0.015

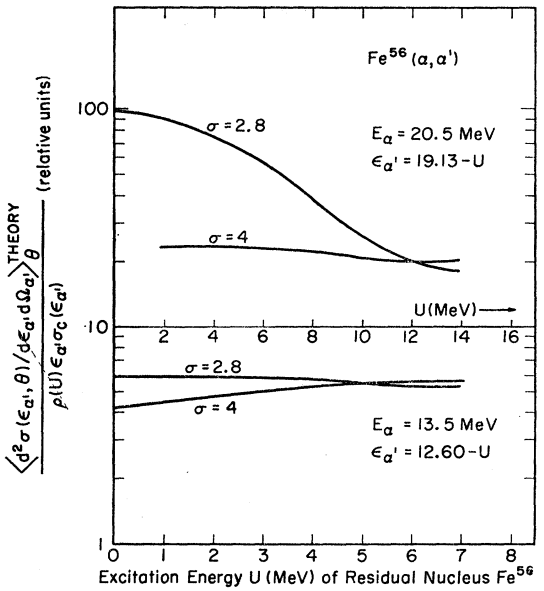

FIG. 10. Deviation of evaporation spectra calculated with exact-statistical and approximate theories [see Eq. (A2)] for the $Fe^{56}(\alpha,\alpha')$ reaction. [See Fig. 3 (caption)].

of the proton-bombarding energy E_p in the laboratory system, the α-particle bombarding energy E_α in the laboratory system, and the spin-cutoff parameter σ. A large number of additional calculations of $A(\epsilon)$ were made for other reactions and a summary of these results in terms of the essential quantity

$$\left\langle \frac{1}{A(\epsilon)} \frac{dA(\epsilon)}{dU} \right\rangle$$

is given in Table IV. The excitation energy U is related to ϵ by Eq. (2). The residual excitation-energy range used to calculate this average is also listed in Table IV. The range in channel energy ϵ of the emitted particles is calculable from Eq. (2). From the results of these calculations some general conclusions can be reached about the validity of the approximate Weisskopf evaporation formula [Eq. (1)] in the mass range 40–70. (1) Equation (1) may be used without correction for analysis of reactions in which the bombarding and emitted particles are both nucleons and the bombarding energy is less than 15 MeV. (2) Sizable deviations from Eq. (1) occur for reactions in which an α particle participates as either bombarding or emitted particle. The biggest deviations may occur when both bombarding and emitted particles are α particles [(α,α') reactions, (see Fig. 10)]. (3) The magnitude of the deviation depends also on the spin-cutoff factor σ, as seen in Fig. 10. If a a large uncertainty exists in this parameter for reactions with higher angular-momentum transfer, it will introduce an uncertainty in the calculated level density.